The Differential Interfacial Tension Hypothesis (DITH): A Comprehensive Theory for the Self-Rearrangement of Embryonic Cells and Tissues

G. Wayne Brodland
e-mail: brodland@uwaterloo.ca
Department of Civil Engineering,
University of Waterloo,
Waterloo ON N2L 3G1,
Canada

A comprehensive theory, herein named the Differential Interfacial Tension Hypothesis (DITH), for the self-rearrangement of embryonic cells and tissues is presented. These rearrangements include sorting, mixing and formation of checkerboard patterns in heterotypic aggregates of embryonic cells, and total or partial engulfment, separation and dissociation of tissues. This broadly-based theory accounts for the action of all currently known cytoskeletal components and cell adhesion mechanisms. The theory is used to derive conditions for the cell and tissue rearrangements named above. Finite element-based computer simulations involving two or more cell types confirm these conditions.
[DOI: 10.1115/1.1449491]

Keywords: Cell Mechanics, Cell Sorting, Cell Mixing, Checkerboard Patterns, Tissue Engulfment, Computer Simulations, Finite Element Method (FEM), Differential Interfacial Tension Hypothesis (DITH), Differential Adhesion Hypothesis (DAH)

Introduction

One of the objects of science is to construct theories that explain natural phenomena. These theories provide a conceptual foundation for analytical and experimental endeavors, and offer an orderly and intellectually satisfying understanding of the physical world. The merit of such theories lies in their simplicity and in their ability to reliably predict a broad range of outcomes.

During the last several decades, numerous theories have been proposed to explain the intriguing mechanical interactions (Fig. 1) that can occur between different types of embryonic cells [1–14]. For example, if a heterotypic aggregate of heart and retinal cells is prepared [7], the cells spontaneously sort. If these two cell types are brought together as homotypic masses [12], the retinal cells spread over the heart cells and the final configuration is similar to that produced by sorting.

For many years, these phenomena have been understood in terms of the Differential Adhesion Hypothesis (DAH) or Steinberg Hypothesis which states that cell motions are driven by differences in the strengths of cell-cell adhesions. The DAH was so widely accepted that it became the *de facto* paradigm, and remained largely unchallenged for three decades. Thus, it is not surprising [15] that new experimental evidence [6,7,10,13,16] and computer simulations [17–23] were almost universally interpreted in terms of the DAH.

When Chen and Brodland were testing a new cell-level finite element formulation [24], they decided to investigate cell sorting because it seemed that this phenomenon was well understood. Although initial tests [25] seemed to support the DAH, a more careful examination found that these and subsequent simulations [26] were in conflict with it. Instead, the simulations led to the conclusion that these cell rearrangements are driven by differences in interfacial tensions. Subsequent studies showed that the physics and experimental literature are not consistent with the DAH but that they are consistent with the concept of interfacial tension-driven rearrangements [14]. These studies laid the foundation for the present work, which embodies the concept of interfacial tension-driven cell rearrangement in a comprehensive theory herein named the Differential Interfacial Tension Hypothesis (DITH), reconciles a wide range of computer simulations carried out by others with the DITH, and investigates aggregates that involve two or more cell types.

The flaw in the concept of adhesion-driven cell rearrangement is difficult to recognize because of widespread confusion about the relationship between the mechanical effect of cell-cell adhesions and that of surface or interfacial tensions. The fundamental and critical difference between them can be understood by considering the cell model shown in Fig. 2(*a*). Microfilaments along the edge of each cell generate a contractile force called F_{MF}, while the contractile force generated by each cell membrane including its associated proteins is called F_{Mem}. In contrast, cell-cell adhesions generate a force F_{Adh} that tends to elongate the intercellular interface since energy is released as new contact is formed [27]. Thus, if two cells, denoted as *L* and *D*, are in contact, the net interfacial tension along their common boundary will be [14]

$$\gamma^{LD} = F^{L}_{\mathrm{Mem}} + F^{D}_{\mathrm{Mem}} + F^{L}_{\mathrm{MF}} + F^{D}_{\mathrm{MF}} - F^{LD}_{\mathrm{Adh}} + F^{LD}_{\mathrm{Other}}, \tag{1}$$

where F^{LD}_{Other} is the net contractile force generated by any other structures whose effects are incorporated into the model. In the case of a cell *L* in contact with the medium, the interfacial tension is actually a surface tension, given by [14]

$$\gamma^{LM} = F^{L}_{\mathrm{Mem}} + F^{L}_{\mathrm{MF}} - F^{LM}_{\mathrm{Adh}} + F^{LM}_{\mathrm{Other}}, \tag{2}$$

where F^{LM}_{Adh} is a generalization of the adhesion concept. Understanding that the force generated by cell-cell adhesions is in the *opposite* direction to that generated by contractile components is critical to eliminating the prevailing confusion. As noted elsewhere [14], the net interfacial tension must be positive, and when the adhesion at a particular interface is increased, the force available to shorten that boundary is reduced.

The DITH and DAH advance different explanations when a medium-surrounded cell aggregate ultimately produces a mass of

Contributed by the Bioengineering Division for publication in the JOURNAL OF BIOMECHANICAL ENGINEERING. Manuscript received by the Bioengineering Division June 7, 2001; revision received December 5, 2001. Associate Editor: C. Dong.

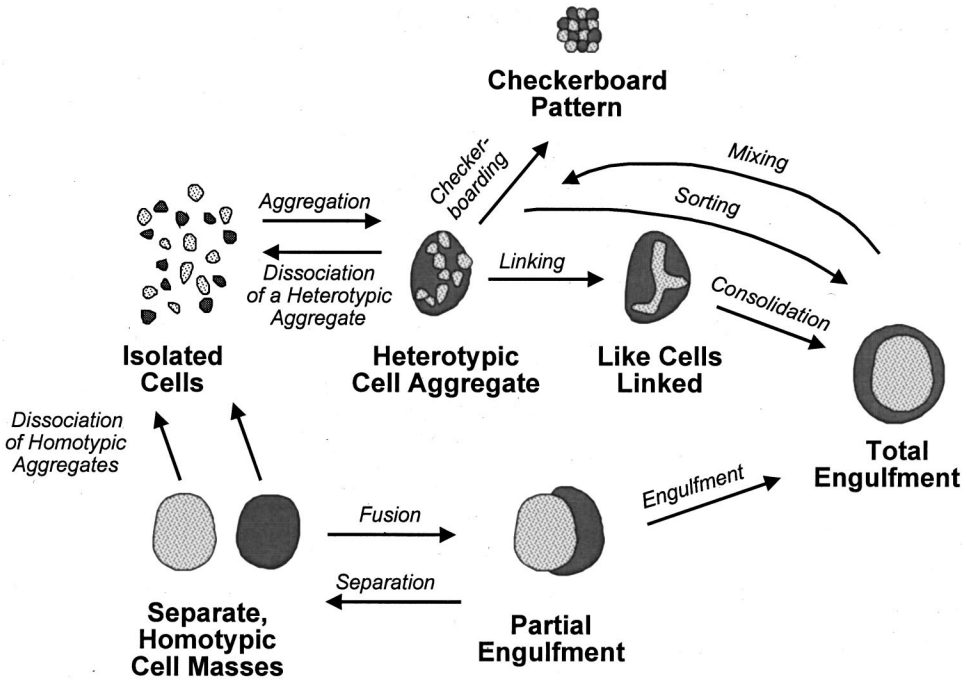

Fig. 1 Phenomena that occur in aggregates of embryonic cells. Expanded from Armstong [12].

type A cells that is completely surrounded by a mass of type B cells. The DITH, and computer simulations that are consistent with it, show that this sorting order can occur if $\gamma^{AM} > \gamma^{BM}$ and that it is guaranteed if $\gamma^{AM} > \gamma^{AB} + \gamma^{BM}$. The DITH also indicates that the strengths of the cohesions are irrelevant, provided that their values do not cause the cells to spontaneously mix or dissociate [14]. This conclusion is inconsistent with the DAH, which states that this pattern would result because the cohesions between type-A cells is greater than the cohesions between type-B cells [7]. Most of the early computer simulations [17–23] are based on an energy minimization principle (which is consistent with the DITH) but, inconsistent with the minus signs in Eqs. (1) and (2), erroneously calculate this energy as the strength of the cell-cell adhesions times the corresponding boundary lengths. When this approach is taken, it leads to the conclusion that the length of the more adhesive boundaries must be more strongly minimized. Strictly speaking, this implies that the more adhesive heterotypic interfaces will preferentially shorten, which on the basis of Eqs. (1) and (2) is exactly opposite to the predictions of the DITH in terms of the strengths of the interfacial tensions and the order of engulfment. Arguments that the more cohesive cells should form the inner mass largely irrelevant since the total length of each type of homotypic interface will be approximately the same regardless of the engulfment order, and so engulfment order does not significantly affect the contributions of the homotypic interfaces to the total system energy. Even so, the DAH has often been seen as a basis for arguing that the cells of the inner mass are more cohesive than those of the outer mass. Since recent experiments in which surface tensions are measured [10,28] show that the pattern of engulfment is consistent with that predicted by the DITH [14], it is difficult to accept arguments [13,28] that the DAH is consistent with surface tension-governed patterns of tissue rearrangement.

The purpose of this paper is to present a comprehensive theory, herein named the Differential Interfacial Tension Hypothesis (DITH), for the self-driven rearrangement of embryonic cells. These rearrangements include the sorting, mixing and formation of checkerboard patterns in heterotypic aggregates of embryonic cells, and the total or partial engulfment of one type of embryonic tissue by another. The theory encompasses the effects of all known cytoskeletal components and cell-cell adhesion mechanisms, including those that depend on particular concentrations of specific molecules [29–33]. Whether these adhesions involve molecular interactions that are homotypic or heterotypic, and regardless of the class of CAM they involve, it would seem that they must all ultimately generate an equivalent normal force which can [24], in turn, be resolved into an equivalent tangential force F_{Adh}^{LD}, allowing their effects to be incorporated into the DITH. The DITH also encompasses all thermodynamically reversible or irreversible and rate-dependent processes that can be considered to contribute to the effective interfacial tensions that act between cells or between cells and a surrounding medium. Other supporting arguments and biological issues associated with the DITH paradigm have been addressed elsewhere [14,24,25].

The DITH is used to derive conditions for a wide range of cell and tissue rearrangements. Finite element-based computer simulations involving two or more cell types are then used to test whether barriers exist that are not predicted by the theory. Without exception, these, and the experimental and computer simulation literature that were thought to support the DAH [14], are found to support the DITH.

Interactions Between Two Cell Types

In an aggregate consisting of two cell types *L* and *D*, four combinations of cell types are possible at any internal triple junction: LLL, LLD, LDD, and DDD. A generic triple junction is illustrated in Fig. 3, where each of the regions labeled *X*, *Y*, and *Z* can be a cell of either type. The figure should be interpreted as a normal cross-section through the three-dimensional curvilinear interface between the three regions.

When three cells of the same type are in contact with each other, the interfacial tensions will be equal to each other, and the junction will tend to move until the angles between each pair of sides is 120 deg. The resulting honeycomb-like pattern or annealed state is well known [16,21,24,26,34,35], and rate constants for this process are currently under investigation. A perfect hon-

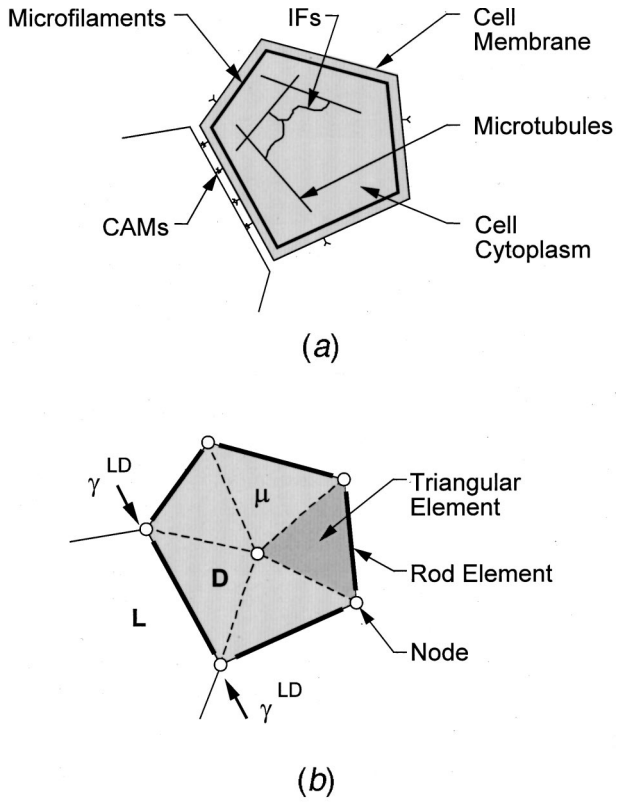

Fig. 2 The cell model. (*a*) Structural components important to cells include microfilaments, microtubules, the cell membrane, cell adhesion molecules (CAMs), the cell cytoplasm and networks of intermediate filaments (IFs). (*b*) The mechanical effects of these components are approximated by an equivalent interfacial tension γ^{LD} and an effective cytoplasmic viscosity μ, and represented, respectively, by rod-like and triangular elements in the finite element model. After Brodland and Chen [26], although in the present context, a cross-section rather than a plan view is intended.

eycomb is not usually attained since the cells do not have identical sizes and their motions may be constrained by boundary conditions.

If the interfacial tensions were negative, the boundaries between the cells would tend to elongate, and ''star-shaped'' cells would result if the edges were constrained to remain straight [36]. In real cells, where this constraint does not exist, they would become convoluted, subject to the bending stiffness of the

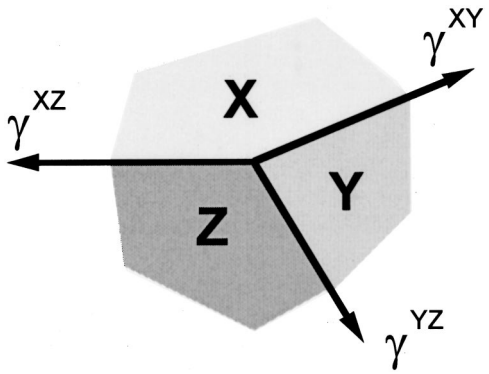

Fig. 3 The forces acting at a generic triple junction

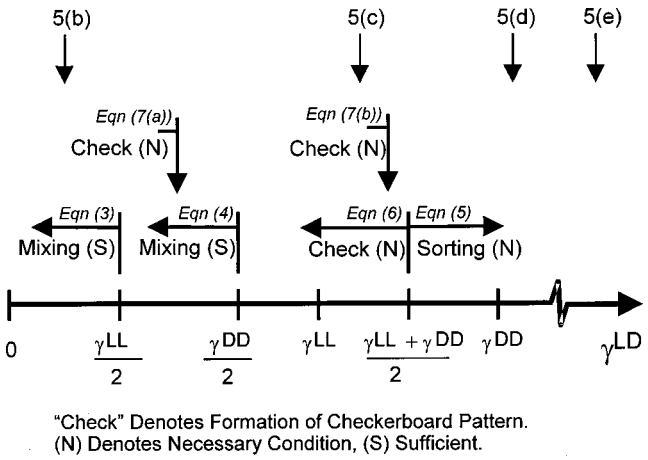

Fig. 4 A summary of the conditions for cell sorting, mixing, and checkerboard-pattern formation. The arrows along the top of the figure indicate where the simulations shown in Fig. 5 fall along the γ^{LD} continuum.

membrane and its associated proteins, much as the boundary between miscible fluids becomes convoluted as a first step in the mixing process [27].

If two cells of one type and one of another are present, a broader range of outcomes is possible. Without loss of generality, consider a triple junction where two type-*L* cells and one type-*D* cell are present. If the tension γ^{LL} is greater than $2\gamma^{LD}$, the net force at the triple junction will be in the general direction of the *L*-*L* interface regardless of the angles formed at the junction, and the *L*-*L* interface will continue to shorten. As this occurs, the type-*D* cell will be drawn in between the type-*L* cells until it wedges them apart, producing mixing of the two cell types. Thus, a sufficient condition on γ^{LD} for mixing is

$$\gamma^{LD} < \frac{\gamma^{LL}}{2} \tag{3}$$

(Fig. 4). A junction with two type-*D* cells and one of type-*L* yields a sufficient condition for type-*L* cells to be drawn between type-*D* cells, namely

$$\gamma^{LD} < \frac{\gamma^{DD}}{2}. \tag{4}$$

In contrast, for sorting to occur, it must be energetically preferable for cells to contact their own kind rather than those of a different kind. Assuming that the formation of new *L*-*D* interface is accompanied by loss of half as much *L*-*L* and *D*-*D* interfaces (the accuracy of this assumption has been confirmed by unpublished finite element simulations), then for energy to be released as cells sort, and heterotypic interfaces are replaced with homotypic ones, it is necessary to have

$$\gamma^{LD} > \frac{\gamma^{LL} + \gamma^{DD}}{2}, \tag{5}$$

where the argument for conversion from energy criteria to force criteria is given below.

In a checkerboard pattern, cells contact those of another type more than those of their own type. For mixed boundaries to be energetically preferable, it is necessary to have the opposite condition,

$$\gamma^{LD} < \frac{\gamma^{LL} + \gamma^{DD}}{2}. \tag{6}$$

Table 1 A comparison of criteria for a variety of cell-cell interactions. The surface energies denoted by *e* and *J* are comparable with the interfacial tensions denoted by γ (see text).

Phenomenon	Present Study (1)	Brodland, 2000 [37]	Graner & Sawada, 1993 [21]	Honda et al., 1986 [20] (2)
Sorting of L and D	$\gamma^{LD} > \frac{\gamma^{LL}+\gamma^{DD}}{2}(N)$	$\gamma^{LD} > \frac{\gamma^{LL}+\gamma^{DD}}{2}(N)$	$e^{LD} > \frac{e^{LL}+e^{DD}}{2}$	
			$e^{LL}+(e^{DM}-e^{LM}) > e^{LD}$	
Mixing of L and D	$\gamma^{LD} < \frac{\gamma^{LL}}{2}(S)$	$\gamma^{LD} < \frac{\gamma^{LL}}{2}(S)$		
	$\gamma^{LD} < \frac{\gamma^{DD}}{2}(S)$	$\gamma^{LD} < \frac{\gamma^{DD}}{2}(S)$		
Checkerboard of L and D	$\gamma^{LD} \cong \frac{1}{\sqrt{2}}\gamma^{LL}(N)$	$\gamma^{LD} < \gamma^{LL}(N)$	$e^{LD} < \frac{e^{DD}+e^{LL}}{2} < 0$	$J^{LD} \cong 2J^{DD} - J^{LL}$
	$\gamma^{LD} \cong \frac{1}{\sqrt{2}}\gamma^{DD}(N)$	$\gamma^{LD} < \gamma^{DD}(N)$		

Additional conditions may also have to be satisfied, as noted in the text. Some of the expressions have been algebraically re-arranged to facilitate comparison.

A vector analysis of the forces at a typical triple junction show that in order to produce the distinctive 90 deg and 135 deg angles characteristic of those patterns usually classified as checkerboards [20,26] the more stringent requirements,

$$\gamma^{LD} \cong \frac{1}{\sqrt{2}}\gamma^{LL} \quad \text{and} \quad \gamma^{LD} \cong \frac{1}{\sqrt{2}}\gamma^{DD} \tag{7}$$

must be satisfied. These criteria are shown in Fig. 4, which is drawn for the case where $\gamma^{DD}/2 < \gamma^{LL}$. The findings are valid regardless of this condition, although the relative positions of some of the criteria will change if this condition is not met.

The above conditions, written in terms of interfacial tensions, are directly comparable to conditions written in terms of surface energy density (Table 1). This comparison is possible because the potential energy of a boundary of length A and unit height that carries a uniform tension γ is γA, equivalent to the energy associated with an interface of the same dimensions that has associated with it an energy density γ. Thus, the energy densities, denoted as J, a, e, and λ by others [18,20–22] can all be interpreted as equivalent to the surface tension γ used here, and as embodying all of the effects represented by Eq. (1). In contrast, the authors of several of these other studies report that the energy densities they use arise from cell-cell adhesions, although they do not assign them negative energy densities as required by Eq. (1). In view of the new arguments presented and referred to here, an interpretation in terms of interfacial tensions is possible and this, in turn, implies that each of these other simulations supports the DITH (Table 1). In contrast to energy formulations, interfacial tensions lend themselves to direct physical interpretation as forces and lead to an understanding of how these cause local force imbalances in specific directions and give rise to corresponding motions. Although Glazier and Graner [22] also use the term surface tension, they point out that in the context of their paper it describes a particular kind of surface energy difference and not a force.

Eqs. (3) to (7) use the DITH to identify conditions for various phenomena. Some of these conditions are based on local interactions at the triple junctions between adjacent cells whereas others are based on more abstract concepts involving energy considerations and average changes in boundary lengths. It remains to be proved that the displacements of triple-junctions predicted by the theory can produce cell rearrangements and the relatively large displacements of entire cells necessary for sorting and other phenomena. The derivations of Eqs. (3) to (7) also do not address a number of other potentially significant factors, such as the relative proportions of the cell types present, the geometry of the starting configuration and the mechanical effects of intracellular pressures.

Computer simulations provide an ideal means to investigate these issues and, here, the finite element formulation of Chen and Brodland [24] is used. This formulation (Fig. 2(*b*)) models the cytoplasm and other structures that fill the area of each n-sided cell using n viscous triangular elements, and uses rod-like elements along each cell boundary to model the net interfacial tension predicted by Eq. (1). Like other formulations used in computer simulations [20–22], this one uses a type of descent method to find a local minimum in the total potential energy of the system. Thus, it would be expected to produce similar patterns of cell behavior compared to those, provided that the surface energies in those simulations are interpreted as interfacial tensions as defined by Eq. (1).

The starting configuration (Fig. 5(*a*)) used for the first series of simulations is a square region within which a regularized Voronoi tessellation [24] was used to generate 200 cells of similar size. The cell types were assigned randomly, as either L (shown with light shading) or D (dark shading). For this set of simulations, γ^{LL} was chosen to have a normalized value [26] of 12 and γ^{DD} was set to 20. This produces an ordering of γ^{LL} and γ^{DD} that is consistent with that shown in Fig. 4. To minimize the effect of the boundary conditions, it was further assumed that mirror images of the patch shown were present along each of its four outside edges. Thus the interfacial tensions along the outside boundaries of the light and dark cells were set, respectively, to 6 and 10—half of the values used for corresponding interior boundaries, since the latter include both sides of the boundary. Values of γ^{LD} were then chosen within each significant range in Fig. 4.

If $\gamma^{LD} = 3$, then both of the mixing criteria (Eqs. (3) and (4)) and the checkerboard criteria (Eq. (6)) are satisfied. However, the checkerboard criteria embodied in Eqs. (7(*a*)) and (7(*b*)) are not satisfied well, and the final configuration that results (Fig. 5(*b*)) is well mixed but not as striking a checkerboard pattern as those reported elsewhere [20,22,26,37]. Additional tests that were carried out show that in regions where cells of any one type form a mass that is more than two cells wide, mixing and checkerboard patterns may not penetrate through the mass.

This example also demonstrates that the "power" of any particular mechanism may be limited, in that it may not be able to generate the predicted effect everywhere from any starting configuration. Like all of the final states presented in Fig. 5, the one shown in part (*b*) corresponds to a local minimum in the potential energy surface. States with lower potential energy apparently exist, but they can only be reached if suitable additional perturbations [22] are applied to the system.

Figure 5(*c*) shows the final configuration produced when γ^{LD}

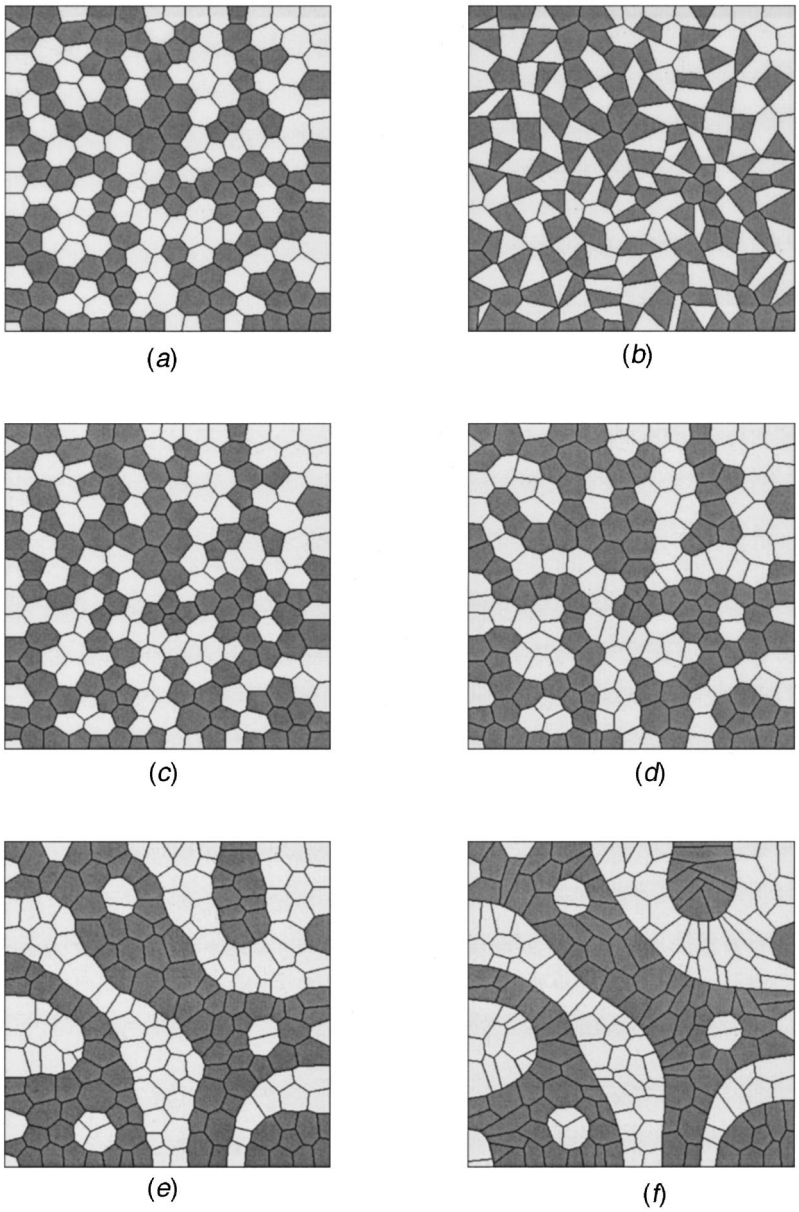

Fig. 5 Some of the phenomena that can occur in a heterotypic planar aggregate. (*a*) Initial configuration with $\gamma^{LL}=12$ and $\gamma^{DD}=20$. (*b*) Total mixing and partial checkerboard ($\gamma^{LD}=3$). (*c*) Partial mixing ($\gamma^{LD}=14$). (*d*) Partial sorting ($\gamma^{LD}=22$). (*e*) Strong sorting, but edges do not release from the boundaries for the reasons described in the text ($\gamma^{LD}=40$). (*f*) Fluid behavior starting from configuration (*e*), as characterized by no tensions along the homotypic interfaces ($\gamma^{LL}=\gamma^{DD}=0$ and $\gamma^{LD}=40$).

$=14$, a value that is just below the minimum for sorting. The result is a tendency to mix, as evidenced by the increased angularity of the light-dark boundary and the separation of a few cells from others of their own kind.

Previous investigations of cell sorting [26] show that cell sorting consists of three steps: the formation of smooth chains, shortening of the chains into approximately round masses, and annealing of the resulting masses. The first sorting case considered here (Fig. 5(*d*)), has γ^{LD} just into the sorting range, and a modest tendency to sort is apparent from the reduced angularity of the light-dark boundaries. When γ^{LD} is increased to 40, there is a much stronger tendency to sort (Fig. 5(*e*)). However, the smooth chains that are formed are not free to round up since their ends do not freely separate from the boundaries of the square. This might be expected since the boundary conditions imply that these chains continue into the reflected copies of the patch assumed to exist along each edge. In other tests (unpublished) manually releasing the chain ends from the edge of the square still does not produce rounding. This behavior, apparently, is due to the highly constrained nature of this set of simulations, as the other two steps associated with sorting do occur in free masses, as shown below. For purposes of comparison, the homotypic tensions γ^{LL} and γ^{DD} were set to zero to simulate a fluid. The geometry shown in Fig. 5(*e*) was used as the starting configuration while the final configuration is shown in Fig. 5(*f*). As might be anticipated, the heterotypic boundaries are as smooth as straight cell edges will permit.

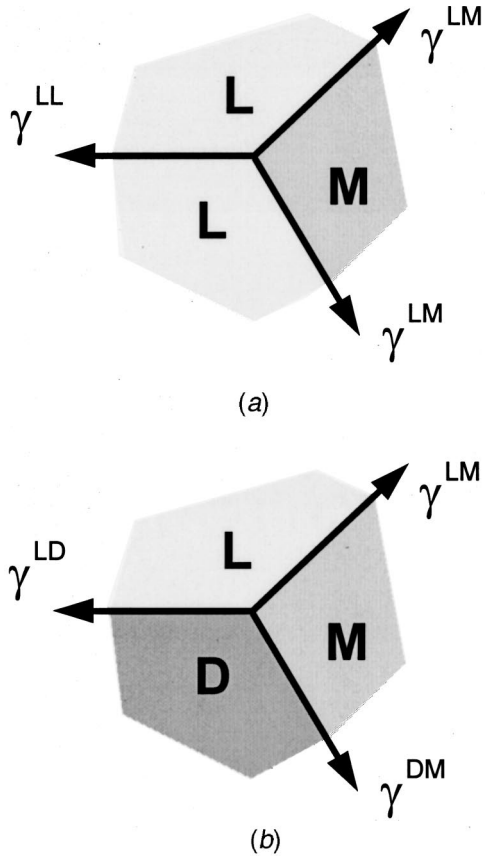

Fig. 6 Triple junctions involving two cells and a medium. Part (*b*) of the figure can be interpreted as two individual cells of types *L* and *D* or as two homotypic cell masses of types *L* and *D*.

Interactions That Involve Cells and the Medium

Similar analyses can be used to investigate triple junctions where medium is present. In that case, two possibilities exist: LLM (or DDM) and LDM. An analysis of a junction between two type-*L* cells and the medium (Fig. 6(*a*)) shows that medium will be drawn in between the cells causing a mass of type-*L* cells to spontaneously dissociate if

$$\gamma^{LL} > 2\gamma^{LM}. \tag{8}$$

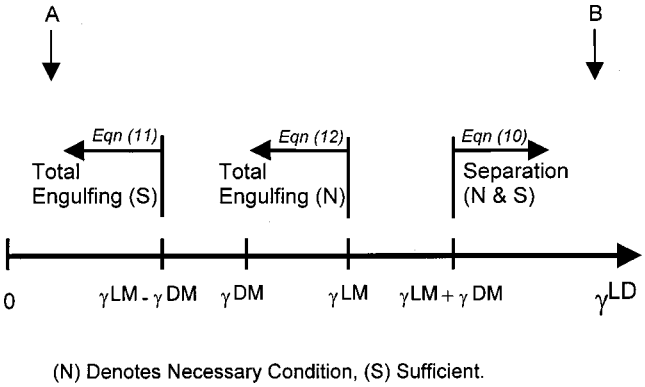

Fig. 7 A summary of the conditions for engulfment and separation of tissues. The arrow marked A corresponds to the simulation shown in Fig. 8, while that marked B corresponds to one in which separation occurs (unpublished) and for which $\gamma^{LM} = \gamma^{DM} = 20$ and $\gamma^{LD} = 150$.

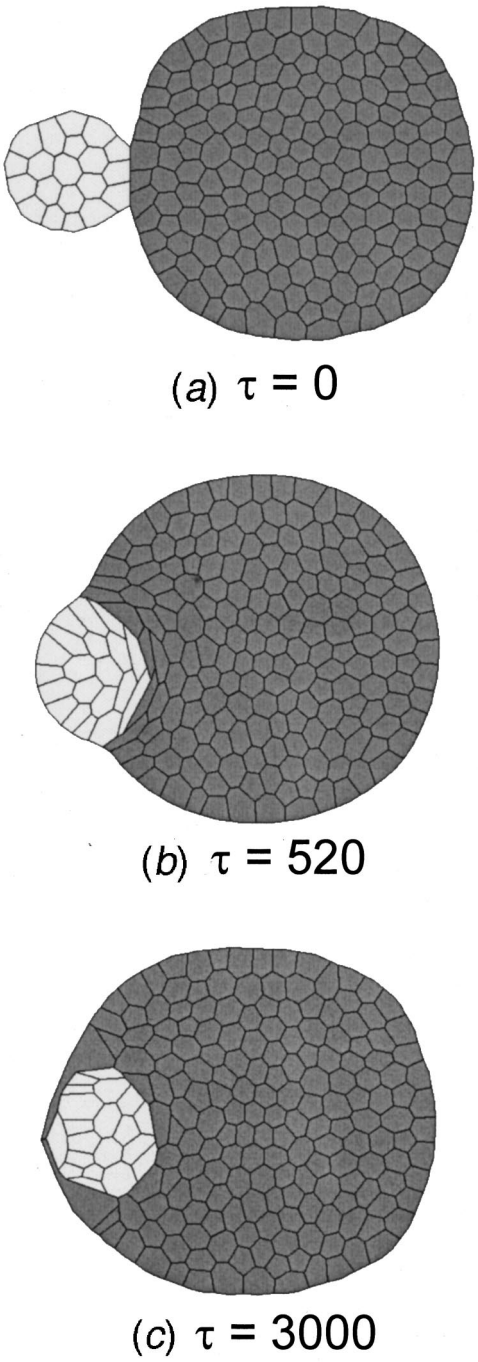

Fig. 8 Total engulfment of one type of tissue (*L*) by another (*D*) ($\gamma^{LL} = \gamma^{DD} = 5$, $\gamma^{LD} = 25$, $\gamma^{LM} = 150$, $\gamma^{DM} = 70$)

A similar analysis shows that a mass of type-*D* cells will be dissociated by a medium if

$$\gamma^{DD} > 2\gamma^{DM}. \tag{9}$$

Additional, unpublished finite element tests confirm these predictions.

A force analysis of a triple junction between cells of types *L* and *D* and the medium (Fig. 6(*b*)) shows that the *L*-*D* boundary will shorten regardless of the angles formed at the junction if

$$\gamma^{LD} > \gamma^{LM} + \gamma^{DM}. \tag{10}$$

Therefore, the medium will be drawn in between the two cell types and they will separate from each other. Thus, Eq. (10) is a

Table 2 A comparison of criteria for cell-cell interactions that involve the surrounding medium. The surface energies denoted by e are comparable with the interfacial tensions denoted by γ (see text).

Phenomenon	Present Study (1)	Brodland & Chen, 2000 [14]	Graner & Sawada, 1993 [21]	Foty & Steinberg, 1995 [10] (2)
Total Engulfment of L by D	$\gamma^{LD} < \gamma^{LM}(N)$ $\gamma^{LD} < \gamma^{LM} - \gamma^{DM}(S)$	$\gamma^{LD} < \gamma^{LM} - \gamma^{DM}(S)$	$e^{LD} < e^{DD} + (e^{LM} - e^{DM})$ $\frac{e^{DD} + e^{LL}}{2} < e^{LD}$	$\gamma^{LD} < \gamma^{LM} - \gamma^{DM}$
Partial Engulfment of L by D	This occurs when neither Total Engulfment nor Separation occur	$\gamma^{LM} - \gamma^{DM} < \gamma^{LD} < \gamma^{LM} + \gamma^{DM}(N)$ $\gamma^{LM} < \gamma^{LD} < \gamma^{DM}(S)$		$\gamma^{LM} - \gamma^{DM} < \gamma^{LD} < \gamma^{LM} + \gamma^{DM}$
Separation of L and D	$\gamma^{LD} > \gamma^{LM} + \gamma^{DM}$ (N & S)	$\gamma^{LD} > \gamma^{LM}(N)$ $\gamma^{LD} > \gamma^{LM} + \gamma^{DM}(S)$	$e^{LD} > e^{LM} + e^{DM}$	$\gamma^{LD} > \gamma^{LM} + \gamma^{DM}$
Dissociation	$\gamma^{LL} > 2\gamma^{LM}(S)$			

Additional conditions may need to be satisfied, as noted in the text. Some formulas shown in terms of surface tensions have been converted from reversible work of adhesion values using formulas contained in Ref. [14]. The formulas shown are for the case where $\gamma^{LM} \leqslant \gamma^{DM}$. When $\gamma^{LM} < \gamma^{DM}$, γ^{LM} and γ^{DM} must be exchanged in some of the formulas so that a positive difference between them results.

sufficient condition for separation. Since, at the moment of pinch-off, the angle between the L and D masses will be very shallow regardless of the relative sizes of the L and D masses, the tension γ^{LD} will be virtually opposed to γ^{LM} and γ^{DM} and Eq. (10) also becomes a necessary condition. Equation (10) is slightly different from the criterion reported elsewhere [14], because the previous work did not recognize that at the moment of pinch-off the interface angles must pass through the limiting case described above. This and the other conditions derived in this section are shown in Fig. 7, which is drawn for the case where $\gamma^{LM} > \gamma^{DM}$.

If the tension along the LM boundary is larger than the sum of the other surface tensions, then type-D cells will be drawn over the type-L cells, regardless of the angles formed at the triple junction, and this sufficient condition can be written in terms of γ^{LD} as

$$\gamma^{LD} < \gamma^{LM} - \gamma^{DM}. \tag{11}$$

If there is a sufficient volume of type D cells, as in Fig. 8(a), the angle between the LD and DM interfaces may approach 90 deg. Then, for engulfment to continue, it is necessary to have

$$\gamma^{LD} < \gamma^{LM}. \tag{12}$$

Similarly, cells of L type will be drawn over those of type D if

$$\gamma^{LD} < \gamma^{DM} - \gamma^{LM}, \tag{13}$$

and engulfment may continue, provided that

$$\gamma^{LD} < \gamma^{DM}. \tag{14}$$

When neither total engulfment nor separation occur, the result is called partial engulfment. The conditions for each of these cases are consistent with the experimental findings summarized in Fig. 4 of Brodland and Chen [14] and generally consistent with the conditions reported there. The conditions reported herein are supported (Table 2) by a large number of computer simulations [20–22,26,37] including that shown in Fig. 8.

In the case of total engulfment, theoretical considerations suggest that the engulfed mass should become perfectly circular in order to reduce the energy of the LD interface. Likewise, the outside of the engulfing mass should become circular. This condition does not actually happen in experiments [12,38] or in computer simulations [22,25,26], apparently because the driving forces are insufficient to cause final rounding of the aggregated masses within a reasonable period of time. There is, however, no theoretical basis for the engulfed mass to become centered within the engulfing mass.

In studies of tissue interactions, the interfacial tensions must be chosen so that cell mixing does not occur when the tissues are brought in contact with each other, and so that the cells in the tissue are not dissociated by the medium.

Aggregates That Involve More Than Two Cell Types

To investigate the mechanics of mixtures that contain more than two types, Voronoi tessellations of 200 cells were made and cells were randomly assigned one of three equiprobable cell types, denoted as being of types light (L), intermediate (I) and dark (D) (Fig. 9(a)). For this simulation, the D-L and D-I pairs satisfy the sorting criteria (Eq. (5)) while the L-I pair satisfies the mixing criterion. As shown in Fig. 9(b) the final configuration is consistent with the individual cell-pair predictions. Numerous other simulations that were carried out using as many as four cell types confirm that the criteria summarized in Fig. 4 describe the interactions between each pair. These findings are consistent with experiments which show that for a set of three real cell types, if two binary systems of them sort, then a mixture made from all three will also sort [13].

Discussion and Conclusions

The basic tenets of the DITH are that net or equivalent surface tensions arise along the edges of cells according to Eqs. (1) and (2). Cell type-specific differences in the values of these tensions give rise to local displacements of triple junctions, which ultimately lead to specific patterns of cell rearrangement. These patterns of rearrangement include those commonly recognized as sorting, mixing, checkerboard pattern formation in heterotypic aggregates, and engulfment, separation and dissociation in tissues. The strengths of these contractions may vary with time in a stochastic or other manner, and the biochemical processes that generate these forces need not be thermodynamically reversible.

If the net equivalent interfacial tension associated with a particular interface depends on whether that interface is increasing or decreasing in length, or if it depends on the rate at which that interface is changing in length, then γ for that interface will not be fixed. In that case, a necessary condition for a particular phenomenon, such as sorting, which involves edge lengthening and shortening would be that all relevant combinations of the interfacial tensions associated with the edge lengthening and shortening processes satisfy the sorting criteria for their typical physiological rates. Variation of interfacial tensions with strain, strain rate, contact area, CAM type and density, and activation may all occur in real cells, and as these effects become quantified, they could be used to adjust the tensions values used in Eqs. (3) to (14), and they could be incorporated into computer simulations. Inasmuch as any forces across the cell boundary can be resolved into tangential and normal components, and since both of these can be converted into equivalent interfacial tensions [14,24], it would seem that all trans-boundary forces can be accommodated by the DITH.

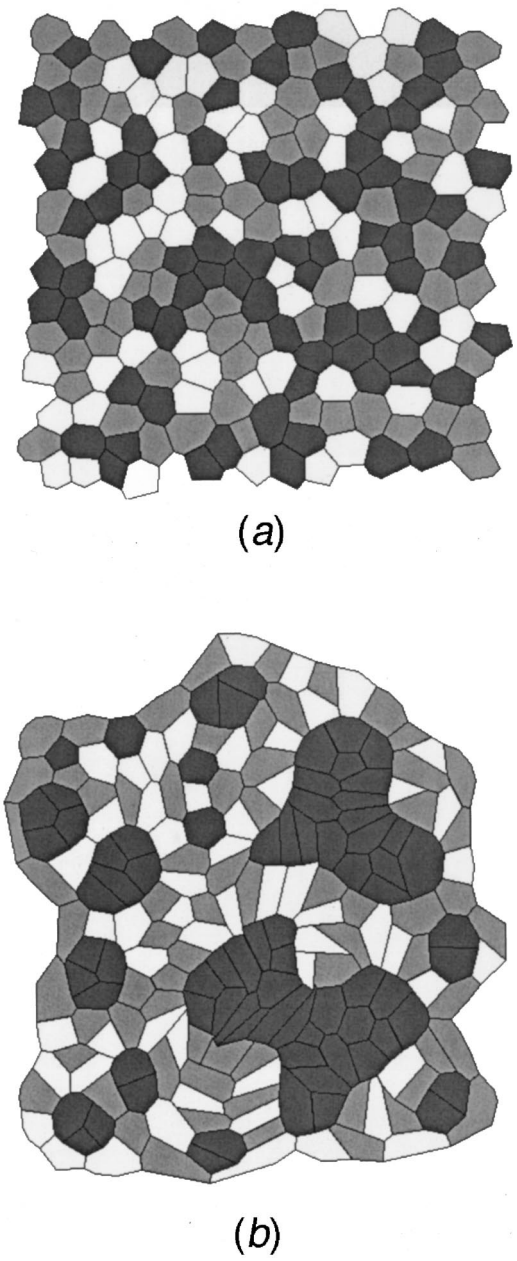

Fig. 9 An aggregate consisting of three cell types. (*a*) Initial configuration of dark (*D*), intermediate (*I*) and light (*L*) cells ($\gamma^{DD}=25$, $\gamma^{II}=\gamma^{LL}=\gamma^{IM}=\gamma^{LM}=20$, $\gamma^{DI}=\gamma^{DL}=50$, $\gamma^{IL}=10$, $\gamma^{DM}=100$). (*b*) Final configuration showing total engulfing of the dark cells by the intermediate and light cells (with one exception), active mixing of the light and intermediate cells with each other, and sorting of the dark cells from the other two types, all as predicted by the theory. The dark cell masses do not totally round up due to mechanical interactions with the surrounding cells.

The DITH is similar to the Differential Surface Contraction Hypothesis (DSCH) proposed by Harris, the boundary shortening model of Honda [34] and a surface tension concept considered briefly by Phillips and Steinberg [35] in that all are based on differential interfacial contractions. The DITH also explains why certain cell behaviors are similar to those produced by immiscible liquids [43–44], a similarity noted by Steinberg [3–5] and others [45]: it is because both are driven by interfacial tensions.

Early experiments suggested that sorting and engulfment might be driven by the same basic mechanism. The present work shows that these plus all of the other phenomena considered here arise from the same basic driving forces. In some cases these forces act at the junctions between trios of cells while in others they act at the junctions between two cells and the medium. For example, when type-*D* cells are drawn in between type-*L* cells, mixing occurs but when medium is drawn in between type-*L* cells mixing of the medium and cells (cell dissociation) occurs. The equations that govern these phenomena (Eqs. (3) and (8), respectively) arise from similar free-body diagrams and can be algebraically manipulated into identical form. Numerous, similar parallels can be demonstrated between the criteria derived here.

The DITH does not rely on any particular mechanisms of force generation, nor does it limit the kinds of force generators that can act. If the mechanisms at work are reversible, they can be incorporated directly into Eqs. (1) and (2). If not, then two versions of these equations must be used, one that describes the forces in edges that are elongating, and another for edges that are shortening. In time, simulations that explicitly model the thermodynamics and specificity of CAMs [11,12,39,40] and other membrane-related proteins may be carried out. Through the concept of equivalent nodal loads, these may provide improved estimates for the forces embodied in Eqs. (1) and (2). This and other studies have highlighted the fact that contractile forces must dominate over adhesive forces [14,26]. However, without the action of cell-cell adhesions, Eq. (1) would not be valid since adjacent cells would simply drift apart and round up separately. Various types of anchoring junctions [41] are also evidently required for similar mechanical reasons.

The DITH is consistent with basic principles of physics and is supported by the experimental literature, though not with traditional interpretations of this literature. It is also supported by a wide variety of computer simulations (Tables 1 and 2), provided that the boundary energies or their equivalents reported therein are re-interpreted as interfacial tensions that arise according to Eqs. (1) and (2). As argued herein, it is important that this literature be re-assessed, with special attention being given to distinguishing between the mechanical effects of interfacial tensions and those of cell-cell adhesions.

The present study also demonstrates that for a particular driving force to be a sufficient cause for a particular outcome, it must be able to drive all of the sequential changes necessary to the outcome. This principle was previously demonstrated in tissue-level finite element simulations of neurulation [42] and in simulations of cell sorting [26]. Here, its application led to more stringent criteria for engulfment and for checkerboard pattern formation than previous studies. Multiple criteria may also have to be satisfied to produce a particular effect. Thus, for example, to produce engulfment, neither cell type must dissociate in the medium, the two cell types must not mix with each other on contact, and the engulfment criteria must be satisfied.

Computer simulations confirm that the DITH is an accurate predictor of specific phenomena, subject to certain limitations. Some of these limitations are due to secondary factors such as the relative amount of each cell type and geometric characteristics of the starting configuration. This suggests that specific geometric conditions may have to be present at the beginning of a particular natural process, as in the quail oviduct cells where the ciliated cells tend to be surrounded by a single layer of gland cells [20]. The simulations also show that when more than two cell types are present, the criteria derived for binary aggregates accurately predict the interactions between each pair. In all cases, the final configurations may not be as easily categorized as published experiments and simulations might imply. To produce distinctive final configurations seems to require finely tuned combinations of interfacial tension values and suitable initial configurations. Unfortunately, experiments in which cells that have been engineered to produce specific interfacial tensions are not yet available. However, the present study is expected to provide a firm foundation for the mechanical design of such experiments. Studies are also be-

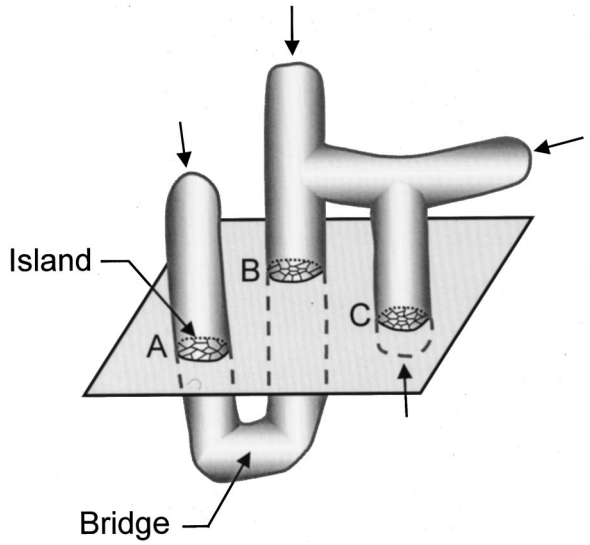

Fig. 10 Sorting in three-dimensions versus two-dimensions. Cells that appear to be isolated islands in a cross-sectional plane or two-dimensional simulation may be connected together by bridges that exist if the third dimension were included. Contraction along the surfaces of such bridges would cause them to shorten and would draw islands such as A and B together, while in other locations taking cells out of the plane, as implied at C.

ginning to appear in which comparisons between simulations and observations of real cells [46] make it possible to extract previously unknown properties.

Early computer simulations showed that sorting in two-dimensional simulations was less complete than in three-dimensional masses of real cells. They also showed that this discrepancy could be eliminated by postulating long-range contractile forces between isolated masses of the same type [18,19,22]. To investigate how groups of cells which appear separated from each other like islands in two dimensions might be connected by bridges in the third dimension (Fig. 10), voxels in a cubic volume were randomly assigned one of two cell types. These studies showed that on average, any one region in the plane was connected to approximately 5 others of the same type. Since the interface between different cell types must be strongly contractile to produce sorting (Eq. (5)), these bridges would draw islands (like *A* and *B*) together and pull cells out of the plane (as at *C*) when they shorten, until a compact mass is formed. Two-dimensional simulations in which contractile bridges were assumed to exist between islands to produce force at a distance confirmed that the islands could be drawn together and the cells made to fuse into a single compact mass.

It should also be noted that cells exhibit a type of motility [47] that is not accounted for by unvarying interfacial tensions, but which can be simulated by varying interfacial tension strengths with time. Additional simulations in which the interfacial tensions were varied with time (unpublished), however, suggested that this was not a significant factor in the class of problems considered herein.

In considering biological phenomena such as those identified in Fig. 1, it is important to remember that ultimately forces must drive all of the necessary shape and conformational changes. Although biochemistry will play an important role in explaining how particular mechanically relevant structures are assembled and regulated, it will always be essential to demonstrate how forces generated at the molecular, cytoskeletal and cellular levels interact in order to produce these phenomena.

In conclusion, the DITH explains a wide range of phenomena, including sorting, mixing and checkerboard pattern formation in cell aggregates and engulfment, separation and dissociation of tissues. It shows that these are indeed all driven by the same basic mechanism, and that this mechanism, namely differential interfacial tensions, is the same as that which drives similar motions in immiscible fluids. It furthermore shows how a wide range of driving forces including the highly specific cell-cell adhesion mechanisms that are currently receiving much attention give rise to these equivalent surface tensions. Thus, the DITH offers a new foundation for further experimental and theoretical studies.

Acknowledgments

The finite element simulations of cells were run by Mr. Jim Veldhuis using software he wrote based on the formulation of Chen and Brodland [24]. Cell meshes were generated and displayed using software written by Mr. Daniel Chen. The theory is an extension of work carried out by Brodland and Chen [14]. The software for the two- and three-dimensional lattice-based studies of connectivity between cell types was written and run by Mr. Alesh Slovak. This research was funded by a Natural Sciences and Engineering Research Council of Canada (NSERC) Research Grant to G.W.B.

References

[1] Townes, P. S., and Holtfreter, J., 1955, ''Directed Movements and Selective Adhesion of Embryonic Amphibian Cells,'' J. Exp. Zool., **128**, p. 53.
[2] Moscona, A., 1960, ''Patterns and Mechanisms of Tissue Reconstruction from Dissociated Cells,'' in *Developing Cell Systems and Their Control*, D. Rudnick, ed., Academic Press, New York, pp. 45–70.
[3] Steinberg, M. S., 1962, ''On the Mechanism of Tissue Reconstruction by Dissociated Cells. I. Population Kinetics, Differential Adhesiveness, and the Absence of Directed Migrations,'' Proc. Natl. Acad. Sci. U.S.A., Vol. **48**, pp. 1577–1582.
[4] Steinberg, M. S., 1962, ''On the Mechanism of Tissue Reconstruction by Dissociated Cells. II. Time-course of Events,'' Science, **137**, pp. 762–763.
[5] Steinberg, M. S., 1962, ''On the Mechanism of Tissue Reconstruction by Dissociated Cells. III. Free Energy Relations and the Reorganization of Fused, Heronomic Tissue Fragments,'' Proc. Natl. Acad. Sci. U.S.A., Vol. **48**, pp. 1769–1776.
[6] Steinberg, M. S., 1970, ''Does Differential Adhesion Govern Self-Assembly Processes in Histogenesis? Equilibrium Configurations and the Emergence of a Hierarchy Among Populations of Embryonic Cells,'' J. Exp. Zool., **173**, pp. 395–434.
[7] Steinberg, M. S., 1975, ''Adhesion-Guided Multicellular Assembly: A Commentary upon the Postulates, Real and Imaged, of the Differential Adhesion Hypothesis, With Special Attention to Computer Simulations of Cell Sorting,'' J. Theor. Biol., **55**, pp. 431–443.
[8] Harris, A., 1975, ''Is Cell Sorting Caused by Differences in the Work of Intercellular Adhesion? A Critique on the Steinberg Hypothesis,'' J. Theor. Biol., **61**, pp. 267–285.
[9] Ohmoro, T., and Maeda, Y., 1986, ''Implications of Differential Chemotaxis and Cohesiveness for Cell Sorting in the Development of Dictyostelium Discoideum,'' Dev., Growth Differ., **28**, pp. 169–175.
[10] Foty, R., and Steinberg, M. S., 1995, ''Liquid Properties of Living Cell Aggregates: Measurement and Morphogenetic Significance of Tissue Interfacial Tensions,'' in *Interplay of Genetic and Physical Properties in the Development of Biological Form*, D. Beysens, G. Forgacs, and F. Gaill, eds., World Scientific, Pub. Co. Pte. Lt., pp. 63–73.
[11] Marrs, J. A., and Nelson, W. J., 1996, ''Cadherin Cell Adhesion Molecules in Differentiation and Embryogenesis,'' Int. Rev. Cytol., **165**, pp. 159–205.
[12] Armstrong, P., 1989, ''Cell Sorting Out: The Self-Assembly of Tissues In Vitro,'' Crit. Rev. Biochem. Mol. Biol., **24**, pp. 119–149.
[13] Steinberg, M. S., 1996, ''Adhesion in Development: An Historical Overview,'' Dev. Biol., **180**, pp. 377–388.
[14] Brodland, G. W., and Chen, H. H., 2000, ''The Mechanics of Cell Sorting and Envelopment,'' J. Biomech., **33**, pp. 845–851.
[15] Kuhn, T., 1962, *The Structure of Scientific Revolutions*, University of Chicago Press, Chicago, IL.
[16] Phillips, H., Steinberg, M. S., and Lipton, B. H., 1977, ''Embroyonic Tissues as Elasticoviscous Liquids II. Direct Evidence for Cell Slippage in Centrifuges Aggregates,'' Dev. Biol., **59**, pp. 124–134.
[17] Antonelli, P. L., Rogers, T. D., and Willard, M. A., 1973, ''Geometry and the Exchange Principle in Cell Aggregation Kinetics,'' J. Theor. Biol., **41**, pp. 1–21.
[18] Goel, N. S., and Rogers, G., 1978, ''Computer Simulation of Engulfment and Other Movements of Embryonic Tissues,'' J. Theor. Biol., **71**, pp. 103–140.
[19] Rogers, G., and Goel, N. S., 1978, ''Computer Simulation of Cellular Movements: Cell-sorting, Cellular Migration Through a Mass of Cells and Contact Inhibition,'' J. Theor. Biol., **71**, pp. 141–166.
[20] Honda, H., Yamanaka, H., and Eguchi, G., 1986, ''Transformation of a Polygonal Cellular Pattern During Sexual Maturation of the Avian Oviduct Epi-

thelium: Computer Simulation,'' J. Embryol. Exp. Morphol., **98**, pp. 1–19.
[21] Graner, F., and Sawada, Y., 1993, ''Can Surface Adhesion Drive Cell Rearrangement? Part II: A Geometrical Model,'' J. Theor. Biol., **164**, pp. 477–506.
[22] Glazier, J., and Graner, F., 1993, ''Simulation of the Differential Adhesion Driven Rearrangement of Biological Cells,'' Phys. Rev. E, **47**, pp. 2122–2154.
[23] Mochizuki, A., Iwasa, Y., and Takeda, Y., 1996, ''A Stochastic Model for Cell Sorting and Measuring Cell-Cell Adhesion,'' J. Theor. Biol., **179**, pp. 129–146.
[24] Chen, H. H., and Brodland, G. W., 2000, ''Cell-Level Finite Element Studies of Viscous Cells in Planar Aggregates,'' ASME J. Biomech. Eng., **122**, pp. 394–401.
[25] Chen, H. H., and Brodland, G. W., 1997, ''Finite Element Simulation of Differential Adhesion-Driven Cell Sorting and Spreading,'' 16th Canadian Congress of Applied Mechanics (CANCAM), L. Cloutier and D. Rancourt, eds., June 1–5, Quebec, pp. 597–598.
[26] Brodland, G. W., and Chen, H. H., 2000, ''The Mechanics of Heterotypic Cell Aggregates: Insights from Computer Simulations,'' ASME J. Biomech. Eng., **122**, pp. 402–407.
[27] Davies, J., and Rideal, E., 1963, *Interfacial Phenomena*, Academic Press, New York.
[28] Foty, R. A., Pfleger, C. M., Forgacs, G., and Steinberg, M. S., 1996, ''Surface Tensions of Embryonic Tissues Predict their Mutual Envelopment Behavior,'' Development, **122**, pp. 1611–1620.
[29] Friedlander, D. R., Mege, R., Cunningham, B. A., and Edelman, G. M., 1989, ''Cell Sorting-Out is Modulated by Both the Specificity and Amount of Different Cell Adhesion Molecules (CAMs) Expressed on Cell Surfaces,'' Proc. Natl. Acad. Sci. U.S.A., Vol. **86**, pp. 7043–7047.
[30] Aplin, A. E., Howe, A. K., and Juliano, R. L., 1999, ''Cell Adhesion Molecules, Signal Transduction and Cell Growth,'' Curr. Opin. Cell Biol., **11**, pp. 737–744.
[31] Huynh-Do, U., Stein, E., Lane, A. A., Liu, H., Cerretti, D. P., and Daniel, T. O., 1999, ''Surface Densities of Ephrin-B1 Determine EphB1-Coupled Activation of Cell Attachment through $\alpha_v\beta_3$ and $\alpha_5\beta_1$ Integrins,'' EMBO J., **18**, pp. 2165–2173.
[32] Petruzzelli, L., Takami, M., and Humes, D., 1999, ''Structure and Function of Cell Adhesion Molecules,'' Am. J. Med., **106**, pp. 467–476.
[33] Xu, Q., Mellitzer, G., Robinson, V., and Wilkinson, D. G., 1999, ''In Vivo Cell Sorting in Complementary Segmental Domains Mediated by Eph Receptors and Ephrins,'' Nature, **399**, pp. 267–271.
[34] Honda, H., 1983, ''Geometrical Models for Cells in Tissues,'' Int. Rev. Cytol., **81**, pp. 191–248.
[35] Phillips, H., and Steinberg, M. S., 1978, ''Embryonic Tissues as Elasticoviscous Liquids I. Rapid and Slow Shape Changes in Centrifuges Cell Aggregates,'' J. Cell. Sci., **30**, pp. 1–20.
[36] Chen, H. H., 1998, ''Finite Element-Based Computer Simulations of Motility, Sorting, and Deformation in Biological Cells,'' Ph.D. thesis, University of Waterloo, Waterloo, Canada.
[37] Brodland, G. W., 2000, ''Conditions for Cell Sorting, Mixing and Checkerboard Pattern Formation Determined Using Mechanics and Computer Simulations,'' 2000 Advances in Bioengineering (BED Vol. 48), (IMECE), Nov. 5–10 Orlando, T. A. Conway, ed., ASME, New York.
[38] Steinberg, M. S., 1963, ''Reconstruction of Tissues by Dissociated Cells,'' Science, **141**, pp. 401–408.
[39] Gumbiner, B. M., 1996, ''Cell Adhesion: The Molecular Basis of Tissue Architecture and Morphogenesis,'' Cell, **84**, pp. 345–357.
[40] Opas, M., 1995, ''Cellular Adhesiveness, Contractility, and Traction: Stick, Grip and Slip Control,'' Biochem. Cell Biol., **73**, pp. 311–316.
[41] Alberts, B., Bray, D., Lewis, J., Raff, M., Roberts, M., and Watson, J., 1997, *Molecular Biology of the Cell*, 2nd Edition, Garland Publishing Inc., New York.
[42] Clausi, D. A., and Brodland, G. W., 1993, ''Mechanical Evaluation of Theories of Neurulation Using Computer Simulations,'' Development, **118**, pp. 1013–1023.
[43] Torza, A., and Mason, S. G., 1969, ''Coalescence of Two Immiscible Liquid Drops,'' Science, **163**, pp. 813–814.
[44] Torza, A., and Mason, S. G., 1970, ''Three-Phase Interactions in Shear and Electric Fields,'' J. Colloid Interface Sci., **33**, pp. 67–83.
[45] Beysens, D. A., Forgacs, G., and Glazier, J. A., 2000, ''Cell Sorting is Analogous to Phase Ordering in Fluids,'' Proc. Natl. Acad. Sci. U.S.A., Vol. **97**, pp. 9467–9471.
[46] Mochizuki, A., Wada, N., Ide, H., and Iwasa, Y., 1998, ''Cell-Cell Adhesion in Limb-Formation, Estimated From Photographs of Cell Sorting Experiments Based on a Spatial Stochastic Model,'' Dev. Dyn., **211**, pp. 204–214.
[47] Mombach, J. C. M., and Glazier, J. A., 1996, ''Single Cell Motion in Aggregates of Embryonic Cells,'' Phys. Rev. Lett., **76**, pp. 3032–3035.